

# ProtFIM: Fill-in-Middle Protein Sequence Design via Protein Language Models

Youhan Lee<sup>1</sup> Hasun Yu<sup>1</sup>

## Abstract

Protein language models (pLMs), pre-trained via causal language modeling on protein sequences, have been a promising tool for protein sequence design. In real-world protein engineering, there are many cases where the amino acids in the middle of a protein sequence are optimized while maintaining other residues. Unfortunately, because of the left-to-right nature of pLMs, existing pLMs modify suffix residues by prompting prefix residues, which are insufficient for the infilling task that considers the whole surrounding context. To find the more effective pLMs for protein engineering, we design a new benchmark, Secondary structureE InFilling rEcoveRy, SEIFER, which approximates infilling sequence design scenarios. With the evaluation of existing models on the benchmark, we reveal the weakness of existing language models and show that language models trained via fill-in-middle transformation, called ProtFIM, are more appropriate for protein engineering. Also, we prove that ProtFIM generates protein sequences with decent protein representations through exhaustive experiments and visualizations.

## 1. Introduction

Optimizing the protein’s function by changing amino acid residues of protein of interest, called protein engineering, has been of great interest in diverse industries such as biofuel (Wen et al., 2009), pharmaceuticals (H Tobin et al., 2014), and agriculture (Rao, 2008). One of the representatives of conventional protein sequence design methods is a mutagenesis technique, which gives evolutionarily plausible protein sequence libraries with the help of genetic engineering (Arnold, 1998). However, this approach requires

substantial efforts from high-throughput screening experiments. Recently, machine learning-guided protein sequence design strategies have been proposed to achieve a more efficient sequence space search using experimentally acquired labeled data (Yang et al., 2019a).

With both advances in high-throughput sequencing technologies and language modeling in the field of natural language processing (NLP), protein language models (pLMs), which are trained in an unsupervised manner using tremendous sets of unlabeled protein sequences (Consortium, 2019), have been developed for generating *de novo* protein sequence (Madani et al., 2020; Hesslow et al., 2022; Moffat et al., 2022; Ferruz et al., 2022; Nijkamp et al., 2022). Existing generative pLMs are trained using an auto-regressive (AR) strategy (Radford et al., 2019; Brown et al., 2020), and generate sequences conditioning on the prefix protein sequences.

Unfortunately, if the target region where we want to change amino acid residues is located at the front, existing pLMs use only a few preceding amino acid residues (“prompts”) for sequence generation. The interaction sites, positions that interact with other proteins or molecules to perform their functions and are mainly modified to improve functionality, are evenly located on the protein sequence. To prove this, we collect 3D protein structures from Protein Data Bank (PDB) database (Sussman et al., 1998) and calculate the relative positions of protein-protein interaction sites on the protein sequences (see details in Appendix A.1). As illustrated in Figure 7, interacting sites are evenly present on the protein sequence. This result suggests that in protein engineering, modifying the amino acid sequence will be done for the middle part of the sequence in many cases. In this case, existing pLMs may not effectively utilize the information behind them, which can result in poor quality of generation.

In this work, we regard middle protein engineering as a fill-in-middle (FIM) sequence generation problem as in Figure 1 and investigate the possibility of pLMs in FIM protein engineering framework. With the emergence of highly accurate protein structure predictors (Jumper et al., 2021; Baek et al., 2021), protein structures are predicted very quickly and accurately at a low cost. Using these advances, we propose a new evaluation scheme, Secondary structurE InFilling

<sup>1</sup>Kakao Brain Corp, Seongnam, Gyeonggi-do, Republic of Korea. Correspondence to: Youhan Lee <youhan.lee@kakaobrain.com>, Hasun Yu <shawn.yu@kakaobrain.com>.

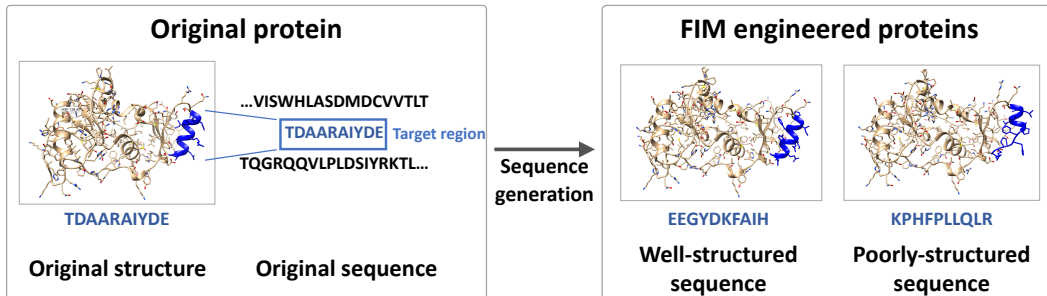


Figure 1. An illustrative example of FIM protein engineering. The changed sequences for the target region are generated by generative pLMs or the like, and the structures are altered accordingly.

rEcoverY, SEIFER, for FIM protein sequence generation. The secondary structures are usually desirable to be preserved (Rubio et al., 2019) since the binding pockets of other interacting proteins or molecules are fixed to some extent. In SEIFER, models are tasked to recommend protein sequences and achieve two conditions: the new sequences must be different from the original sequences and their secondary structures must be fully maintained. So, SEIFER can assess both the diversity and structure of new sequences simultaneously and we believe that SEIFER is suitable for assessing generated sequences in the field of protein engineering which modifies the amino acid residues of original sequences to improve functions. Also, inspired by the latest research in the field of language models (Bavarian et al., 2022b), we propose a new Protein language model specialized for the Fill-In-Middle task, ProtFIM. Compared to existing pLMs, our proposed ProtFIM uses both front (“prefix”) and back (“suffix”) sequence information during training and inference.

Through SEIFER evaluation, we prove that ProtFIM outperforms AR-based pLM, ProtGPT2-C, in infilling protein sequence design. In addition, compared to state-of-the-art released models that were trained with 2-50 times more parameters, ProtFIM exhibits comparable performance, demonstrating the efficacy of infilling modeling in protein engineering. Intriguingly, we discovered that existing pLMs are proficient at only  $\alpha$ -helix engineering, whereas their performances on  $\beta$  and coil structures are similar or worse compared to the random generator, which randomly generates protein sequences for target sites. Furthermore, we provide ablation studies of the  $\alpha$ -helix SEIFER performance on the relative positions and lengths of target sites, demonstrating that only ProtFIM consistently performs better than the random mutation. In addition, using protein fitness prediction tasks, we demonstrate that infilling modeling can give a better representation than existing pLMs with a similar number of parameters. Lastly, case studies show that ProtFIM generates promising sequences, proving the effectiveness

of infilling modeling in real-world protein engineering. In summary, our contributions are:

- We define FIM protein engineering as protein sequence infilling tasks and provide the applicability of pLMs on the task.
- We propose a new evaluation scheme, SEIFER, that can be used to evaluate the performance of pLMs on protein infilling sequence design tasks by considering structural conservation.
- We propose a new type of pLM, ProtFIM, that has both AR and FIM capability. Comprehensive results show that ProtFIM has efficient and comparable performances in protein infilling and protein representations for protein engineering compared to other pLMs.
- We show that the ProtFIM acts as a sequence optimizer, which generates novel sequences with high pLDDT of AlphaFold2 while maintaining the structures essential for the function of the protein.

## 2. Related Work

**Protein language models** Pretraining-based language modelings such as Transformer (Vaswani et al., 2017), BERT (Devlin et al., 2018), and GPT (Ferruz et al., 2022) have revolutionized natural language processing and shown remarkable performance on various tasks such as language understanding, sentence generation, and infilling over the last few years. With a huge increase in the amount of unlabeled protein sequences (Consortium, 2019) produced by high throughput sequencing technologies, pLMs have been introduced and resolved the challenges in protein science and engineering by learning protein languages. BERT-style models primarily provide protein embeddings to solve prediction problems, including protein structure prediction (Rao et al., 2020; Jumper et al., 2021; Lin et al., 2022),

function prediction (Brandes et al., 2022), and property prediction (Rives et al., 2021). GPT-style architectures are utilized in resolving generation challenges such as protein sequence design (Madani et al., 2020; Hesslow et al., 2022; Moffat et al., 2022; Ferruz et al., 2022; Nijkamp et al., 2022).

**Protein sequence design** Attempts to efficiently design protein sequences can be divided into two categories: a method for conducting a large number of high-throughput experiments with mutagenesis and a machine learning-based sequence generation method. Recent advances in experimental-based methods (Fowler & Fields, 2014) allow us to assess the functional changes of mutated protein sequences at a large scale and produce a lot of labeled data. Many machine learning-based sequence design methods generate the optimized sequences iteratively based on the feedback of labeled data (Yang et al., 2019a; Xu et al., 2020; Wu et al., 2021; Shin et al., 2021). Unfortunately, both approaches require a lot of cost and effort in experiments. Recently, several works generate protein sequences conditioned on given 3D structures using a single energy function (Alford et al., 2017), convolutional neural networks (Zhang et al., 2020; Qi & Zhang, 2020), graph neural networks (Ingraham et al., 2019; Jing et al., 2020; Strokach et al., 2020; Dauparas et al., 2022), or Transformers (Hsu et al., 2022). Since these works require 3D coordinate information to generate sequences, generation may be limited only to areas where high-quality structures exist. Also, in these works, CATH (Orengo et al., 1997) is used to evaluate how similar the generated sequences are to the original sequence. This evaluation method may not be suitable for protein engineering, which aims to change the sequence to have a better function. In parallel, generative pLMs such as RITA (Hesslow et al., 2022), DARK (Moffat et al., 2022), ProtGPT2 (Ferruz et al., 2022), and Progen2 (Nijkamp et al., 2022) have been developed. These generative pLMs generate protein sequences having well-folded and viable structures even though these methods do not employ any structural information. However, due to the nature of the AR model itself, these methods utilize only the preceding sequence information during sequence generation. Our proposed ProtFIM has both AR and FIM properties, resulting in efficient FIM protein engineering.

### 3. Method

**Problem Setup** In NLP, infilling is defined as generating complete text  $x$  given incomplete text  $\tilde{x}$ , including one or more missing spans. Similarly, we can regard protein engineering on middle residues as an infilling task where models are tasked to return new protein sequences  $s$  given incomplete protein sequence  $\tilde{s}$  containing missing residues on the target region. Additionally, in the protein infilling task, there is a special structure conservation constraint where

the secondary structure of the target site is maintained to approximate the protein engineering scenario properly. Taken together, our goal is to develop a pLMs,  $f(\tilde{s}; \theta)$ , which outputs complete protein sequence  $s$  based on a distribution  $p(s|\tilde{s})$  and sequence  $s$  must have different residues while having the same secondary structure as that of the original residues.

#### 3.1. Model requirements

Language modeling that learns patterns of raw sequences includes masked language modeling (MLM), causal language modeling (CLM), permutation language modeling (PLM), and infilling language modeling (ILM), all of which have achieved great success for specific applications. Therefore, it is crucial to select a model that best fits the characteristics of the system to be solved, so defining essential requirements of the target system is preemptive to adopting the model. We suggest four key characteristics of pLMs suitable for protein infilling tasks as follows:

- (1) **Dynamic property:** The model can handle various lengths of protein sequences because the lengths of the middle sites are diverse depending on various applications.
- (2) **Generation considering the surrounding context:** The structure and function of proteins are determined through complex interactions between amino acids and atoms constituting the amino acids. Therefore, sequence generation must be conducted considering the contexts around the infilling site to be optimized.
- (3) **Efficiency:** Various strategies, such as pre-processing training data, modifying the model architecture, and using special tokens for controlling, can be used. However, these approaches must be fulfilled as efficiently as possible because the protein sequence length is relatively long (we use the maximum length of residues as 1024 in this work).
- (4) **Diversity:** Because there are many combinations giving the same secondary structures, pLMs that generate diverse sequences different from existing sequences are preferred.

For the protein infilling sequence generation, an MLM-based non-AR method is a good option considering (2) and (3) but is relatively weak in (1) and (4). On the other hand, CLM has shown strengths in (1) and (4) but has weaknesses in (2) and (3). PLM satisfies (1), (2), and (4), but there are computation costs during training in terms of (3). Recently, many works have revealed that infilling training using a simple input transformation enables full-context conditioning generation in an existing AR model. From this point of

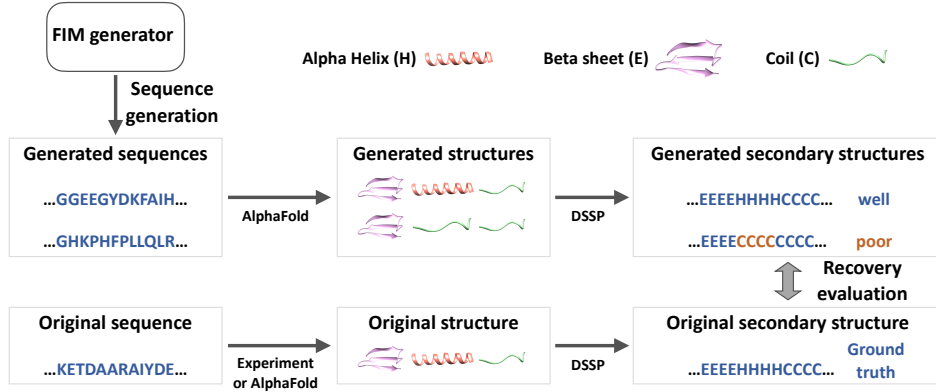


Figure 2. Illustration of our SEIFER evaluation scheme, which estimates the recovery rates of the secondary structures of the generated structure for the original secondary structure.

view, we believe that this infilling modeling will overcome the weaknesses of the AR model (2) and (3) to obtain a model suitable for the protein infilling task. Conventionally, infilling modeling uses unique tokens (Aghajanyan et al., 2022; Donahue et al., 2020), and we use an efficient infilling approach using the latest technique, fill-in-middle transformation (Bavarian et al., 2022a).

### 3.2. Model development

**FIM training** In FIM transformation, a span of text from the middle of a whole sentence is moved to its end, and additional special tokens are introduced for marking where spans are from. The transformation is stochastically fulfilled during causal language modeling training. Intriguingly, this simple and straightforward transformation successfully gives fill-in-the-middle (FIM) capability to the model without modifying model architecture and sacrificing left-to-right causal generation capacity. The transformation is easily applied to protein sequence modeling as follows. First, we tokenize each residue  $R$  of a protein sequence  $S$  with length  $N$  to the sequence consisting of corresponding tokens  $T$  (see eqn. 1 and 2).

$$S = (R_1, R_2, \dots, R_N) \quad (1)$$

$$S_t = (T_1, T_2, \dots, T_N) \quad (2)$$

Second, we conduct uniform sampling to get the start position  $K$  of the middle span of length  $L$  and add special tokens [PRE], [MID], and [SUF] at the beginning of each prefix, middle, and suffix part, respectively. Finally, FIM-transformed sentences are created by concatenating prefix, suffix middle in order as eqn. 3.

$$S'_t = ([PRE], R_1, \dots, R_{K-1}, [SUF], R_{K+L+1}, \dots, R_N, [MID], R_K, \dots, R_{K+L}) \quad (3)$$

Because several residues are needed to form a secondary structure, the middle residue sampling is conducted so that both prefix and suffix parts have at least four residues. The traditional GPT2 architecture from Hugging Face (Wolf et al., 2019) is used for training, and FIM transformation is applied to the input with a 50% frequency. We denote pLMs trained using FIM transformation as ProtFIM in this work. More details are written in Appendix A.4.

**FIM inference for middle residue engineering** For generating complete sequences in protein infilling tasks, we consider the target region as the middle part, and the front and back regions of the target region are prefixes and suffixes. Then, we make a prompt for FIM generation by concatenating the prefix part, suffix part, and [MID] token as eqn. 4.

$$P'_t = ([PRE], R_1, \dots, R_{K-1}, [SUF], R_{K+L+1}, \dots, R_N, [MID]) \quad (4)$$

## 4. Experiments

Section 4.1 illustrates our proposed evaluation scheme, SEIFER, specially designed for protein infilling tasks. Section 4.2 describes metrics and various baseline models covering representative language modeling approaches such as causal language modeling (CLM) and permutation language modeling (PLM). Section 4.3 includes evaluation results of SEIFER tasks. Then, section 4.4 and 4.4 provide ablation studies of the SEIFER task concerning the relative position and length of the target region. Additionally, other metrics for evaluating pLMs, such as perplexity and sequence recovery, are provided in Appendix A.6.



#### 4.1. Evaluation

**Protein secondary structure** Protein secondary structures play a key role as an intermediate between the primary sequences and functional tertiary structures that determines the function of proteins in a variety of biological process. Therefore, designing properly optimized combinations of residues having the same secondary structures can lead to enhanced function of protein (Rubio et al., 2019). Protein secondary structures are categorized into regular and irregular categories. First, the regular structure includes  $\alpha$ -helix (H),  $\beta$ -sheet (E) (Pauling et al., 1951), and the irregular structure type is a coil (C). In this work, we adopt a 3-class secondary structure definition and those structures are calculated via DSSP (Kabsch & Sander, 1983).

**Protein secondary structure recovery via infilling** In this work, we propose a new evaluation scheme, Secondary structurE InFilling rEcoveRy, SEIFER, evaluating the sequence generation and structure conservation simultaneously. In the task, first, models are tasked to generate various sequences to fill the provided target sites. Since secondary structures are calculated based on three-dimensional structural information, the characterization of tertiary protein structures for each generated sequence must be preceded. Unfortunately, conducting experimental characterization on all the new sequences is practically impossible. Instead of this, we utilize AlphaFold2 (Jumper et al., 2021), which has shown near-experiments prediction performance, to predict tertiary structures of all generated sequences. Then, secondary structures of each new sequence are calculated via DSSP algorithm using DSSP module of Biopython (Cock et al., 2009). Finally, the secondary structures of new sequences are compared to the original secondary structures. We assign a positive value, 1, in the case where all new residues have the same secondary structure as the original sequences. And all other cases are negative, 0. We illustrate the process of SEIFER in Figure 2. We use proteins presented in CASP14 to obtain candidate middle sites for SEIFER tasks. And, we argue that our experimental setting is reliable because AlphaFold2 was stringently assessed and proved by remarkable prediction performance on the proteins in the CASP14. Additionally, we use the middle sites, which have minimum lengths of 10, 6, and 6 for helix, beta, and coil structures, respectively, considering the average number of residues for the structures.

**Difference of SEIFER over protein residue recovery task** Sequence recovery has been widely used to evaluate the generation performance of protein generative language models (Ingraham et al., 2019). However, considering that the objective of sequence optimization is to design new sequences with better target properties, recovery of original residues would not be proper. So, a metric is needed to eval-

uate whether the model can generate a variety of sequences while maintaining the function of the protein. Because the function of protein is directly linked to local structure, evaluating the model ability that generates different residues with the same local structure is a promising way. So, we argue that our proposed SEIFER tasks are appropriate for simulating sequence engineering scenarios, because in SEIFER tasks models are tasked to recover the protein’s local structure, especially, secondary structures, not residues.

#### 4.2. Experimental setup

**Baseline** We compare our ProtFIM with other pLMs covering diverse generation strategies. First, for a fair comparison, we train ProtFIM and ProtGPT2-C using the same data and optimization steps. Both models learn protein sequence at the character level, namely, the residue level. To approximate the conventional mutagenesis method, we employ a random generator, which randomly samples amino acids at target locations. Additionally, we employ publicly released other PLMs used as baselines. Specifically, we select ProGen2 as a representative AR PLMs, a concurrently released suite of AR pLMs with various parameters from 151M to 2.7B. Because XLNet (Yang et al., 2019b) can consider both prefix and suffix information during inference because of permutation language modeling, we also employ the publicly released ProtXLNet model, a variant of XLNet for protein (Elnaggar et al., 2022) as another PLMs considering full-context.

**Evaluation metrics** SEIFER measures how many sequences with the same secondary structure exist among new sequences created by a generative model. It is like a retrieval or recommendation engine for protein sequences. In the SEIFER task, all models generate K sequences for N middle sites, and all sequences are evaluated by whether the whole secondary structures at each target site are recovered. If the whole secondary structures are recovered, it is a true positive (TP). Then, Precision@K is the mean of TP/K for N sites. Also, we use Retrieval@K, which assumes a positive case where any true positive sequence exists in generated K sequences, zero otherwise. Thus, Retrieval@K is (the number of sites having TP among K)/N.

#### 4.3. Experimental results on SEIFER tasks

**Retrieval-view** As shown in Table 1, ProtFIM performs better than ProtGPT2-C regarding retrieval. Considering the fact that both models are trained with the same data, hyperparameters, and number of parameters, with the exception of the fill-in-middle transformation, these results indicate that conditioning on both prefixes and suffixes is necessary for improved sequence design in protein engineering. Interestingly, ProtFIM also outperforms the existing PLMs, which are trained with 2-20 times larger weights via CLM and

Table 1. Model performances on SEIFER tasks in terms of retrieval.

MODEL	#PARAMS	OBJECTIVE	H ( $\alpha$ -HELIX)		E ( $\beta$ -SHEET)		C (COIL)		H	E	C	ALL AVG
			R@3	R@5	R@3	R@5	R@3	R@5	AVG	AVG	AVG	
PROGEN2-SMALL	151M	CLM	0.59	0.71	0.67	0.64	0.69	0.80	0.65	0.71	0.75	0.70
PROGEN2-MEDIUM	764M	CLM	0.54	0.66	0.69	0.79	0.70	0.79	0.60	0.74	0.75	0.70
PROGEN2-LARGE	2.7B	CLM	0.59	0.64	0.70	0.79	0.69	0.82	0.62	0.75	0.76	<b>0.71</b>
PROTXLNET	409M	PLM	0.61	0.69	0.66	0.75	0.66	0.76	0.65	0.71	0.71	0.69
RANDOM GENERATOR	-	-	0.46	0.60	0.76	0.82	0.76	0.80	0.53	0.79	0.78	0.70
PROTGPT2-C	85M	CLM	0.58	0.66	0.71	0.79	0.69	0.74	0.62	0.75	0.72	0.70
PROTFIM (OURS)	85M	FIM	0.57	0.71	0.74	0.82	0.74	0.81	0.64	0.78	0.78	<b>0.73</b>

Table 2. Model performances on SEIFER tasks in terms of precision.

MODEL	#PARAMS	OBJECTIVE	H ( $\alpha$ -HELIX)		E ( $\beta$ -SHEET)		C (COIL)		H	E	C	ALL AVG
			P@3	P@5	P@3	P@5	P@3	P@5	AVG	AVG	AVG	
PROGEN2-SMALL	151M	CLM	0.32	0.32	0.45	0.43	0.47	0.48	0.32	0.44	0.48	0.41
PROGEN2-MEDIUM	764M	CLM	0.31	0.32	0.45	0.47	0.49	0.47	0.32	0.46	0.48	0.42
PROGEN2-LARGE	2.7B	CLM	0.36	0.34	0.44	0.45	0.50	0.51	0.35	0.45	0.51	<b>0.43</b>
PROTXLNET	409M	PLM	0.37	0.36	0.42	0.42	0.49	0.49	0.37	0.42	0.49	<b>0.43</b>
RANDOM GENERATOR	-	-	0.25	0.25	0.49	0.47	0.47	0.45	0.25	0.48	0.46	0.40
PROTGPT2-C	85M	CLM	0.31	0.31	0.48	0.47	0.45	0.45	0.31	0.48	0.45	0.41
PROTFIM (OURS)	85M	FIM	0.31	0.32	0.45	0.46	0.48	0.48	0.32	0.46	0.48	<b>0.42</b>

PLM. In particular, 2B-parameterized ProGen-Large has an average retrieval score of 0.71, but 85M-parameterized ProtFIM has a higher score of 0.73. In addition, ProtFIM is superior to ProtXLNet, which is another PLMs that construct sequences based on their surrounding contexts. This indicates that infilling achieves both efficiency and effectiveness.

**Precision-view** Table 2 includes the SEIFER scores in terms of precision. We find that ProtFIM continues to outperform ProtGPT2-C. Contrary to the retrieval-view, existing PLMs shows strong performance. However, we see that ProtFIM exhibits the same score of 0.42 as ProGen2-medium, which is nine times larger than ProtFIM, highlighting the importance of considering pre- and post-context surrounding target sites again.

**Comparison to random mutation** Intriguingly, we discover that current PLMs perform similarly to or worse than the random generator under certain situations. To explore these empirical results, we calculated secondary structure recovery scores for each of the three secondary structures. Interestingly, we find that all PLMs noticeably outperform the random generator only for the  $\alpha$ -helix, but not for the coils and beta sheets. To analyze the finding, we check the distribution of secondary structures for the proteins with known structures by calculating the distribution of secondary structures in proteins from PDB (details are described in Appendix A.2). Figure 8 depicts 3-classes and 4-classes secondary structure distribution, demonstrating that the  $\alpha$ -helix structures are dominant in natural protein structures. This empirical result is consistent with the widely

known observation in the protein community. We hypothesize that this imbalance gives undesirable  $\alpha$ -helix bias in existing protein sequence datasets. Additionally, the coil usually has unordered noisy structures. Taking the above facts together, it is reasonable to conclude that the similar or worse performances of pLMs in  $\beta$ -sheets and coil to the random generator are reasonable because helix bias makes it difficult for models to learn the rules of generating residues consisting of the coil and  $\beta$ -sheet.

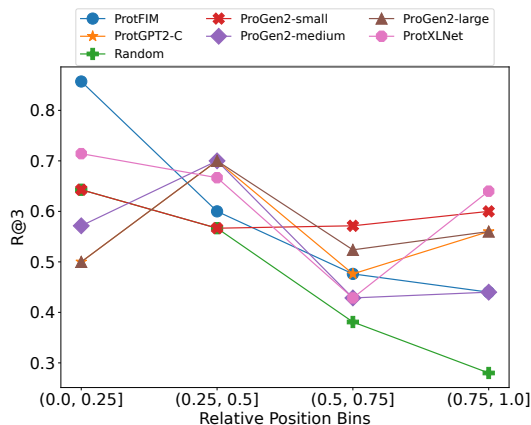


Figure 3. Performance changes in the term of retrieval with regard to (a) relative positions of middle sites.

#### 4.4. Ablation study and analysis

**Change upon the position of target region** We start with an assumption that previous AR pLMs would be ineffective in FIM protein engineering because the sequence generation of AR pLMs is fulfilled by conditioning on only prefix residues. To verify whether this phenomenon occurs, we ablate the SEIFER performance concerning the relative position of the target middle sites. After dividing each protein sequence into four parts, the  $\alpha$ -helix recovery performances of each model corresponding to each part are averaged and illustrated in Figure 3. Interestingly, we observe that only ProtFIM consistently better performances compared to the random generator. Specifically, in the first part (front part), only two models, ProtFIM and ProtXLNet, which take both prefix and suffix parts into account outperform the random generator, but AR PLMs such as ProtGPT2-C and ProGen-series do not. These results confirm our hypothesis. Additionally, the fact that ProtFIM beats ProtXLNet in the front part proves the effectiveness of the FIM training scheme because ProtFIM has five times fewer parameters than ProtXLNet. Meanwhile, PLMs are generally better than the random generator in other parts, indicating the effectiveness of pLMs on protein middle engineering. In addition, the performance of the model is not uniform over positions. We think that it is due to the lack of an evaluation dataset because the number of used CASP proteins is 28. However, since the models are compared under the same conditions, the insight obtained from the performance comparison in the experiments is reliable.

**Change upon the length of target region** We can see that the random generator shows comparable performances to pLMs in several tasks in the above results. To investigate this phenomenon, we ablate the SEIFER performances according to the length of the middle sites. We partition the range of lengths into four parts, and plot corresponding averaged Recall@K as in Figure 4. Interestingly, the random generator performs similarly to pLMs in the first quarter (short length size). However, the performance of the random generator drastically drops as the length of the target sites becomes longer, and it fails all predictions when the middle sites are longer than 30. Meanwhile, the performance of pLMs degrades gradually and fails at the last part, where the middle sites are longer than 40. All the results imply that the length of the middle sites is the main factor for model performance. We explain this using the degree of freedom on possible protein structures of target middle sites. Since the high-dimensional interactions between amino acids make the structure of the protein, the structure is determined to some extent by the structural context from other residues except residues of the middle sites. In other words, the degree of freedom in the structure of the middle sites is relatively small due to the non-target residues. Considering that any

amino acid is a building block of a  $\alpha$ -helix,  $\beta$ -sheet, and coil structure, even if the amino acid is randomly sampled, there will be a high probability of obtaining the desired original structure in FIM scenarios. Meanwhile, the observation that pLMs still work at the longer middle sites shows that pLMs would be a promising solution for long FIM protein sequence design, giving efficient sequence search compared to random generator.

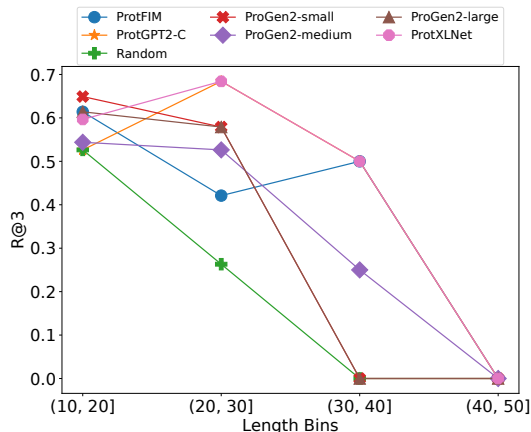


Figure 4. Performance changes in the term of retrieval with regard to (a) relative length of middle sites.

**Representation quality** Collecting experimental functional properties of protein sequence gives insights into a sequence-to-function relationship called fitness landscape. In protein engineering, the fitness landscape is used to rank designed sequences. To this end, pLMs can provide sequence representation for fitness prediction. Recently, FLIP benchmarks have been introduced to assess the quality of representations of pLMs (Dallago et al., 2021). Using FLIP, we compare the embeddings of ProtFIM with baselines. Additionally, ESM-1b and 1v (Rao et al., 2020) are added to compare FIM with masked language modeling (MLM). In FLIP, embeddings of sequences are directly used to predict fitness without fine-tuning pLMs. For a fair comparison, embeddings are obtained via averaging of all residue representations.

Table 3 shows that ProtFIM has strong protein representations over ProtGPT2-C, meaning that infilling modeling benefits representation learning because the modeling considers surrounding contexts that AR PLMs can not deal with. When comparing the existing pLMs, ProtFIM has decent performance. We note that the reason we conduct this experiment is not to show SOTA performance but to show that infilling modeling can improve the representation quality of AR modeling. In summary, the results prove that infilling modeling via FIM transformation gives PLMs both decent

Table 3. Zero-shot fitness prediction on FLIP tasks. All scores are Spearman correlation.

MODEL	#PARAMS	OBJECTIVE	AAV	GB1	MELTOME	META AVG.
ESM-1B (MEAN)	750M	MLM	0.36	0.34	0.71	0.47
ESM-1V (MEAN)	750M	MLM	0.33	0.38	0.72	0.48
ProGEN2-SMALL	151M	CLM	0.39	-0.21	0.56	0.25
ProGEN2-MEDIUM	764M	CLM	0.18	-0.11	0.59	0.22
ProGEN2-LARGE	2.7B	CLM	0.41	0.24	0.68	0.44
PROTXLNET	409M	PLM	0.33	0.29	0.47	0.36
PROTGPT2-C	85M	CLM	0.40	0.18	0.53	0.37
PROTFIM	85M	FIM	0.39	0.25	0.60	<b>0.41</b>

representation and FIM ability. Detailed scores are included in Appendix A.8

## 5. Sequence design analysis

### 5.1. pLDDT change

AlphaFold2 gives a per-residue confidence metric called the predicted local distance difference test (pLDDT) ranging from 0 to 100. Recently, several works have used this metric as a scoring criterion to assess designed protein sequences by assuming that the higher pLDDT, the better and more plausible structure (Moffat et al., 2022; Wang et al., 2022). To assess the FIM engineering performance of models in terms of pLDDT, we collect all pLDDT scores of all created structures in SEIFER and compute the differences of pLDDT between designed structures and corresponding original structures. Finally, we visualize the difference using a cumulative density plot. We compare ProtFIM with ProtGPT2-C to provide a fair comparison. Figure 5 reveals that ProtFIM has the largest positive cases, where pLDDT increases ( $\Delta pLDDT > 0$ ), compared to both ProtGPT2-C and random mutation, demonstrating the specialty of ProtFIM in real-world protein sequence optimization.

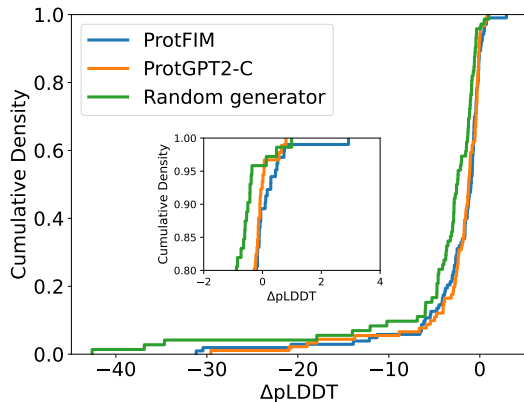


Figure 5. Cumulative density plot on pLDDT change.

### 5.2. Case study

We cherry-pick a protein and visualize the original and modified structures through ProtFIM as shown in Figure 6. The new two sequences of middle sites are different from the original sequences, but all have  $\alpha$ -helix. Interestingly, in-depth visualization considering the side-chain unveils the subtle difference, resulting in well or poorly-optimized sequences. All the above results demonstrate that our model can serve as a sequence design framework, which optimizes the target sequence while maintaining the structures.

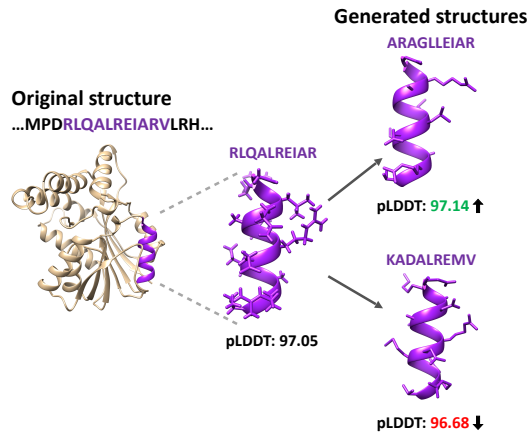


Figure 6. An example of a case where pLDDT increases or decreases after protein sequence design via ProtFIM.

## 6. Conclusion

In this work, we have empirically verified the weakness of the existing AR PLMs and the effectiveness of infilling modeling in real-world protein engineering. Through our proposed new evaluation scheme, SEIFER, we show that a new type of protein language model, ProtFIM, performs protein middle sequence design efficiently compared to existing pLMs. Additional analysis and visualization also prove that ProtFIM is a promising tool for practical protein engineering such as fitness prediction and sequence optimization.



## References

- Aghajanyan, A., Huang, B., Ross, C., Karpukhin, V., Xu, H., Goyal, N., Okhonko, D., Joshi, M., Ghosh, G., Lewis, M., et al. Cm3: A causal masked multimodal model of the internet. *arXiv preprint arXiv:2201.07520*, 2022.
- Alford, R. F., Leaver-Fay, A., Jeliaskov, J. R., O’Meara, M. J., DiMaio, F. P., Park, H., Shapovalov, M. V., Renfrew, P. D., Mulligan, V. K., Kappel, K., et al. The rosetta all-atom energy function for macromolecular modeling and design. *Journal of chemical theory and computation*, 13(6):3031–3048, 2017.
- Arnold, F. H. Design by directed evolution. *Accounts of chemical research*, 31(3):125–131, 1998.
- Baek, M., DiMaio, F., Anishchenko, I., Dauparas, J., Ovchinnikov, S., Lee, G. R., Wang, J., Cong, Q., Kinch, L. N., Schaeffer, R. D., et al. Accurate prediction of protein structures and interactions using a three-track neural network. *Science*, 373(6557):871–876, 2021.
- Bavarian, M., Jun, H., Tezak, N., Schulman, J., McLeavey, C., Tworek, J., and Chen, M. Efficient training of language models to fill in the middle. *arXiv preprint arXiv:2207.14255*, 2022a.
- Bavarian, M., Jun, H., Tezak, N., Schulman, J., McLeavey, C., Tworek, J., and Chen, M. Efficient training of language models to fill in the middle. *arXiv preprint arXiv:2207.14255*, 2022b.
- Brandes, N., Ofer, D., Peleg, Y., Rappoport, N., and Linial, M. Proteinbert: A universal deep-learning model of protein sequence and function. *Bioinformatics*, 38(8):2102–2110, 2022.
- Brown, T., Mann, B., Ryder, N., Subbiah, M., Kaplan, J. D., Dhariwal, P., Neelakantan, A., Shyam, P., Sastry, G., Askell, A., et al. Language models are few-shot learners. *Advances in neural information processing systems*, 33:1877–1901, 2020.
- Bryant, D. H., Bashir, A., Sinai, S., Jain, N. K., Ogden, P. J., Riley, P. F., Church, G. M., Colwell, L. J., and Kelsic, E. D. Deep diversification of an aav capsid protein by machine learning. *Nature Biotechnology*, 39(6):691–696, 2021.
- Cock, P. J., Antao, T., Chang, J. T., Chapman, B. A., Cox, C. J., Dalke, A., Friedberg, I., Hamelryck, T., Kauff, F., Wilczynski, B., et al. Biopython: freely available python tools for computational molecular biology and bioinformatics. *Bioinformatics*, 25(11):1422–1423, 2009.
- Consortium, U. Uniprot: a worldwide hub of protein knowledge. *Nucleic acids research*, 47(D1):D506–D515, 2019.
- Dallago, C., Mou, J., Johnston, K. E., Wittmann, B. J., Bhattacharya, N., Goldman, S., Madani, A., and Yang, K. K. Flip: Benchmark tasks in fitness landscape inference for proteins. *bioRxiv*, 2021.
- Dauparas, J., Anishchenko, I., Bennett, N., Bai, H., Ragotte, R. J., Milles, L. F., Wicky, B. I., Courbet, A., de Haas, R. J., Bethel, N., et al. Robust deep learning-based protein sequence design using proteinmpnn. *Science*, pp. eadd2187, 2022.
- Devlin, J., Chang, M.-W., Lee, K., and Toutanova, K. Bert: Pre-training of deep bidirectional transformers for language understanding. *arXiv preprint arXiv:1810.04805*, 2018.
- Donahue, C., Lee, M., and Liang, P. Enabling language models to fill in the blanks. *arXiv preprint arXiv:2005.05339*, 2020.
- Elnaggar, A., Heinzinger, M., Dallago, C., Rehawi, G., Wang, Y., Jones, L., Gibbs, T., Feher, T., Angerer, C., Steinegger, M., Bhowmik, D., and Rost, B. Prottrans: Toward understanding the language of life through self-supervised learning. *IEEE Transactions on Pattern Analysis and Machine Intelligence*, 44(10):7112–7127, 2022. doi: 10.1109/TPAMI.2021.3095381.
- Ferruz, N., Schmidt, S., and Höcker, B. Protgpt2 is a deep unsupervised language model for protein design. *Nature communications*, 13(1):1–10, 2022.
- Fowler, D. M. and Fields, S. Deep mutational scanning: a new style of protein science. *Nature methods*, 11(8):801–807, 2014.
- H Tobin, P., H Richards, D., A Callender, R., and J Wilson, C. Protein engineering: a new frontier for biological therapeutics. *Current drug metabolism*, 15(7):743–756, 2014.
- Hesslow, D., Zanichelli, N., Notin, P., Poli, I., and Marks, D. Rita: a study on scaling up generative protein sequence models. *arXiv preprint arXiv:2205.05789*, 2022.
- Hsu, C., Verkuil, R., Liu, J., Lin, Z., Hie, B., Sercu, T., Lerer, A., and Rives, A. Learning inverse folding from millions of predicted structures. *bioRxiv*, 2022.
- Ingraham, J., Garg, V., Barzilay, R., and Jaakkola, T. Generative models for graph-based protein design. *Advances in neural information processing systems*, 32, 2019.
- Jarab, A., Kurzawa, N., Hopf, T., Moerch, M., Zecha, J., Leijten, N., Bian, Y., Musiol, E., Maschberger, M., Stoeck, G., et al. Meltome atlas—thermal proteome stability across the tree of life. *Nature methods*, 17(5):495–503, 2020.

- Jing, B., Eismann, S., Suriana, P., Townshend, R. J., and Dror, R. Learning from protein structure with geometric vector perceptrons. *arXiv preprint arXiv:2009.01411*, 2020.
- Jumper, J., Evans, R., Pritzel, A., Green, T., Figurnov, M., Ronneberger, O., Tunyasuvunakool, K., Bates, R., Žídek, A., Potapenko, A., et al. Highly accurate protein structure prediction with alphafold. *Nature*, 596(7873):583–589, 2021.
- Kabsch, W. and Sander, C. Dictionary of protein secondary structure: pattern recognition of hydrogen-bonded and geometrical features. *Biopolymers: Original Research on Biomolecules*, 22(12):2577–2637, 1983.
- Kingma, D. P. and Ba, J. Adam: A method for stochastic optimization. *arXiv preprint arXiv:1412.6980*, 2014.
- Lin, Z., Akin, H., Rao, R., Hie, B., Zhu, Z., Lu, W., dos Santos Costa, A., Fazel-Zarandi, M., Sercu, T., Candido, S., et al. Language models of protein sequences at the scale of evolution enable accurate structure prediction. *bioRxiv*, 2022.
- Loshchilov, I. and Hutter, F. Decoupled weight decay regularization. *arXiv preprint arXiv:1711.05101*, 2017.
- Madani, A., McCann, B., Naik, N., Keskar, N. S., Anand, N., Eguchi, R. R., Huang, P.-S., and Socher, R. Progen: Language modeling for protein generation. *arXiv preprint arXiv:2004.03497*, 2020.
- Moffat, L., Kandathil, S. M., and Jones, D. T. Design in the dark: Learning deep generative models for de novo protein design. *bioRxiv*, 2022.
- Nijkamp, E., Ruffolo, J., Weinstein, E. N., Naik, N., and Madani, A. Progen2: exploring the boundaries of protein language models. *arXiv preprint arXiv:2206.13517*, 2022.
- Orengo, C. A., Michie, A. D., Jones, S., Jones, D. T., Swindells, M. B., and Thornton, J. M. Cath—a hierarchical classification of protein domain structures. *Structure*, 5(8):1093–1109, 1997.
- Pauling, L., Corey, R. B., and Branson, H. R. The structure of proteins: two hydrogen-bonded helical configurations of the polypeptide chain. *Proceedings of the National Academy of Sciences*, 37(4):205–211, 1951.
- Qi, Y. and Zhang, J. Z. Denscpd: improving the accuracy of neural-network-based computational protein sequence design with densenet. *Journal of chemical information and modeling*, 60(3):1245–1252, 2020.
- Radford, A., Wu, J., Child, R., Luan, D., Amodei, D., Sutskever, I., et al. Language models are unsupervised multitask learners. *OpenAI blog*, 1(8):9, 2019.
- Rao, A. G. The outlook for protein engineering in crop improvement. *Plant physiology*, 147(1):6–12, 2008.
- Rao, R., Meier, J., Sercu, T., Ovchinnikov, S., and Rives, A. Transformer protein language models are unsupervised structure learners. *Biorxiv*, 2020.
- Rives, A., Meier, J., Sercu, T., Goyal, S., Lin, Z., Liu, J., Guo, D., Ott, M., Zitnick, C. L., Ma, J., et al. Biological structure and function emerge from scaling unsupervised learning to 250 million protein sequences. *Proceedings of the National Academy of Sciences*, 118(15):e2016239118, 2021.
- Rubio, M. V., Terrasan, C. R. F., Contesini, F. J., Zubieta, M. P., Gerhardt, J. A., Oliveira, L. C., de Souza Schmidt Gonçalves, A. E., Almeida, F., Smith, B. J., De Souza, G. H. M. F., et al. Redesigning n-glycosylation sites in a gh3  $\beta$ -xylosidase improves the enzymatic efficiency. *Biotechnology for biofuels*, 12(1):1–14, 2019.
- Shin, J.-E., Riesselman, A. J., Kollasch, A. W., McMahon, C., Simon, E., Sander, C., Manglik, A., Kruse, A. C., and Marks, D. S. Protein design and variant prediction using autoregressive generative models. *Nature communications*, 12(1):1–11, 2021.
- Strokach, A., Becerra, D., Corbi-Verge, C., Perez-Riba, A., and Kim, P. M. Fast and flexible protein design using deep graph neural networks. *Cell systems*, 11(4):402–411, 2020.
- Sussman, J. L., Lin, D., Jiang, J., Manning, N. O., Prilusky, J., Ritter, O., and Abola, E. E. Protein data bank (pdb): database of three-dimensional structural information of biological macromolecules. *Acta Crystallographica Section D: Biological Crystallography*, 54(6):1078–1084, 1998.
- Suzek, B. E., Wang, Y., Huang, H., McGarvey, P. B., Wu, C. H., and Consortium, U. Uniref clusters: a comprehensive and scalable alternative for improving sequence similarity searches. *Bioinformatics*, 31(6):926–932, 2015.
- Vaswani, A., Shazeer, N., Parmar, N., Uszkoreit, J., Jones, L., Gomez, A. N., Kaiser, Ł., and Polosukhin, I. Attention is all you need. *Advances in neural information processing systems*, 30, 2017.
- Wang, J., Lisanza, S., Juergens, D., Tischer, D., Watson, J. L., Castro, K. M., Ragotte, R., Saragovi, A., Milles, L. F., Baek, M., et al. Scaffolding protein functional sites using deep learning. *Science*, 377(6604):387–394, 2022.

- Wen, F., Nair, N. U., and Zhao, H. Protein engineering in designing tailored enzymes and microorganisms for biofuels production. *Current opinion in biotechnology*, 20(4):412–419, 2009.
- Wolf, T., Debut, L., Sanh, V., Chaumond, J., Delangue, C., Moi, A., Cistac, P., Rault, T., Louf, R., Funtowicz, M., et al. Huggingface’s transformers: State-of-the-art natural language processing. *arXiv preprint arXiv:1910.03771*, 2019.
- Wu, N. C., Dai, L., Olson, C. A., Lloyd-Smith, J. O., and Sun, R. Adaptation in protein fitness landscapes is facilitated by indirect paths. *Elife*, 5:e16965, 2016.
- Wu, Z., Johnston, K. E., Arnold, F. H., and Yang, K. K. Protein sequence design with deep generative models. *Current opinion in chemical biology*, 65:18–27, 2021.
- Xu, Y., Verma, D., Sheridan, R. P., Liaw, A., Ma, J., Marshall, N. M., McIntosh, J., Sherer, E. C., Svetnik, V., and Johnston, J. M. Deep dive into machine learning models for protein engineering. *Journal of chemical information and modeling*, 60(6):2773–2790, 2020.
- Yang, K. K., Wu, Z., and Arnold, F. H. Machine-learning-guided directed evolution for protein engineering. *Nature methods*, 16(8):687–694, 2019a.
- Yang, Z., Dai, Z., Yang, Y., Carbonell, J., Salakhutdinov, R. R., and Le, Q. V. Xlnet: Generalized autoregressive pretraining for language understanding. *Advances in neural information processing systems*, 32, 2019b.
- Zhang, Y., Chen, Y., Wang, C., Lo, C.-C., Liu, X., Wu, W., and Zhang, J. Prodconn: Protein design using a convolutional neural network. *Proteins: Structure, Function, and Bioinformatics*, 88(7):819–829, 2020.

## A. Appendix

### A.1. Interaction sites extraction

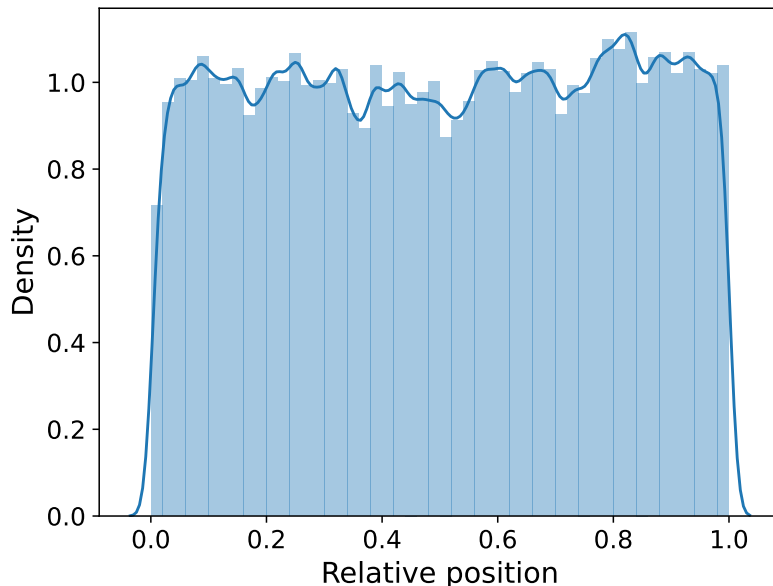


Figure 7. Relative positions of the interacting sites on the protein sequences.

We download 3D protein structures from PDB database (Sussman et al., 1998) and extract protein structures satisfying several conditions: having more than two protein chains; having UniProt ID and a length of the entire sequence in mmCIF dictionaries from MMCIF2Dict module of Biopython (Cock et al., 2009). We hypothesize that the two residue pairs of two different chains would be involved in the interaction if any atom excluding hydrogen of the residues were at a Euclidean distance of  $8\text{\AA}$  or less. Then, we identify all residues which are likely to be involved in the interactions and find where these residues are located on the entire protein sequence.

### A.2. Secondary structure statistics

We analyze the secondary structures of 166,512 structures that can be processed through a DSSP module of Biopython. Biopython classifies the secondary structures as eight classes by default: alpha helix (4-12) (code: 'H'), isolated beta-bridge residue (code: 'B'), strand (code: 'E'), 3-10 helix (code: 'G'), pi helix (code: 'I'), turn (code: 'T'), bend (code: 'S'), and none (code: '-'). In our study, The eight classes are mapped to the three classes as follows: 'H', 'G', and 'I' are mapped to the  $\alpha$ -helix class 'H'; 'B' and 'E' are mapped to the  $\beta$ -sheet class 'E'; 'T', 'S', 'C', and '-' are mapped to the coil class 'C'. In addition, in the right part of Figure 8, '-' is displayed separately.

Figure 8 shows that  $\alpha$ -helix substructures are dominant in natural proteins, meaning imbalance. Furthermore, coil structures have rules that are difficult to capture. Therefore, the model trained using the existing natural protein database would be familiar with the  $\alpha$ -helix generation. Therefore, a preprocessing or encoding technique that can alleviate the  $\alpha$ -helix bias can be a good research topic in the future.

### A.3. Training datasets

For training, protein sequences from UniRef50 (Suzek et al., 2015) dated March 28, 2018 version are used to avoid leakage of CASP13, 14 and conduct a fair comparison with other models. 5% of protein sequences in the UniRef50 are randomly selected as a held-out validation set. The total number of sequences in training data is 25M.



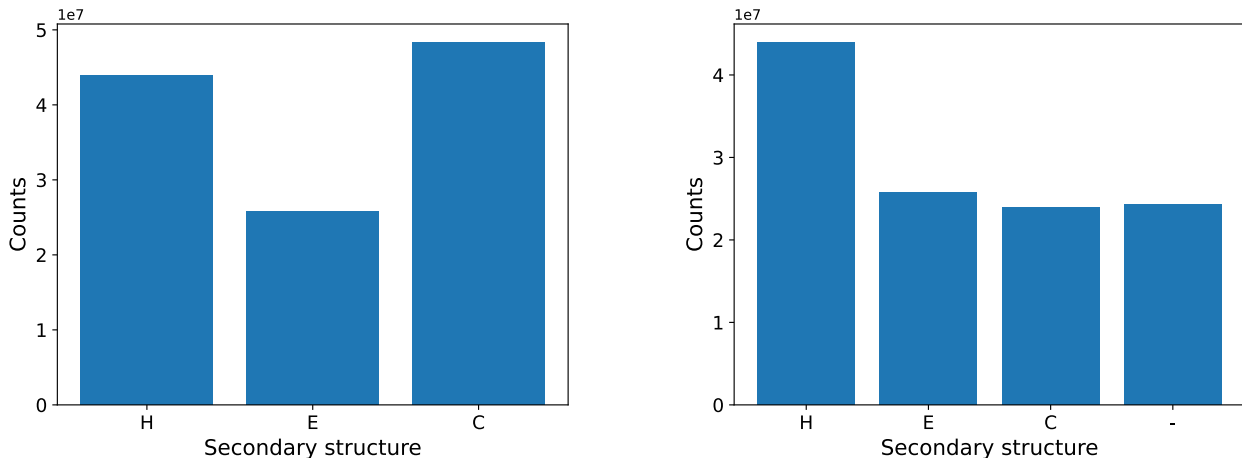


Figure 8. Secondary structure distribution of proteins in PDB database. H, E, C, and - correspond to  $\alpha$ -helix,  $\beta$ -sheet, coil, and none-type. Left: describes 3-classes secondary structure distribution. Right: because coil can be divided into two categories, the coil and none-type structure in DSSP algorithm, we can calculate a 4-classes distribution.

#### A.4. Training details

ProtFIM is trained with a batch size of 128. The maximum length of each protein sequence we used for training is 1024. For ProtFIM optimization, we use AdamW optimizer (Kingma & Ba, 2014; Loshchilov & Hutter, 2017) with a weight decay ratio of  $1e-5$ . The learning rate is scheduled using cosine-warmup strategy. The total optimization step is 500k with 1k warmup steps. We train the model on 8 NVIDIA A100s in 4 days. FIM transformation is applied with 50% of probability. The model consists of 12 layers with a feature dimension of 768. The architecture is based on the released GPT2-base model by HuggingFace (Wolf et al., 2019).

#### A.5. Generation hyper-parameters

We conduct sequence generation using HuggingFace generation API. The topK and topP values are set to 100 and 0.95. We set the temperature as 1.0. After sequence generation, we select top-K sequences. If shorter sequences are generated compared to the length of middle sites, we increase topK by 10 and conduct generation until K sentences are collected. We use the default option of HuggingFace API for other hyper-parameters. These hyper-parameters and generation processes are applied on ProtFIM, ProtGPT2, and ProGen2 models for a fair comparison. Also, we use ProtXLNet to generate sequences of target sites auto-regressively with conditioning on bidirectional context using topK sampling as other AR models.

#### A.6. Perplexity and sequence recovery

We also add other evaluation metrics, such as perplexity and sequence recovery rates, which are widely used for evaluating language models in inverse folding. Table 4 shows the result of perplexity and sequence recovery rates. ProtFIM performs poorly in terms of perplexity and sequence recovery rates. In the FIM paper (Bavarian et al., 2022b), some experiments find that perplexity alone is insufficient for evaluating the infilling task because infilling is conducted in a somewhat different nature compared to conventional left-to-right generation as expressed like  $P_{FIM}(M | P, S) > P_{AR}(M | P)$  where P, M, S indicate prefix, middle, and suffix part, respectively.

Additionally, our targeted infilling task aims to design various sequences in the presence of local structure constraints considering the surrounding context, which is quite different from restoring residues as much as possible. So, there needs to be an appropriate evaluation scheme simulating protein middle engineering tasks that change amino acid residues of local parts of the protein to optimize the target protein, such as enzymes and antibodies. So, sequence residue recovery rate, a widely used metric to evaluate models' sequence design performance, is insufficient for the protein infilling task. Based on the above results and descriptions, we argue that our proposed SEIFER tasks are more appropriate for evaluating protein

Table 4. Perplexity and sequence recovery rates.

MODEL	#PARAMS	OBJECTIVE	PERPLEXITY ( $\downarrow$ )	RECOVERY RATE (%) ( $\uparrow$ )
ProGen2-SMALL	151M	CLM	16.88	8
ProGen2-MEDIUM	764M	CLM	16.17	10
ProGen2-LARGE	2.7B	CLM	16.24	9
ProTxlNet	409M	PLM	16.58	8
ProTgpt2-C	80M	CLM	17.08	8
ProtFIM	80M	FIM	17.04	9

Table 5. Zero-shot fitness prediction on adeno-associated virus (AAV) capsid proteins (Bryant et al., 2021). All scores are Spearman correlation.

MODEL	#PARAMS	OBJECTIVE	MUT-DES	DES-MUT	1-VS-REST	2-VS-REST	7-VS-REST	LOW-VS-HIGH	AVG.
ESM-1B (MEAN)	750M	MLM	0.63	0.59	0.04	0.26	0.46	0.18	0.36
ESM-1V (MEAN)	750M	MLM	0.55	0.44	0.18	0.16	0.45	0.20	0.33
ProGen2-SMALL	151M	CLM	0.38	0.53	0.39	0.47	0.43	0.14	0.39
ProGen2-MEDIUM	764M	CLM	0.19	0.25	0.14	0.30	0.22	0.00	0.18
ProGen2-LARGE	2.7B	CLM	0.68	0.67	0.33	0.20	0.42	0.13	0.41
ProTxlNet	409M	PLM	0.55	0.58	0.21	0.02	0.42	0.20	0.33
ProTgpt2-C	85M	CLM	0.59	0.66	0.24	0.34	0.41	0.16	0.40
ProtFIM	85M	FIM	0.53	0.56	0.32	0.24	0.44	0.28	0.39

infilling tasks than existing metrics such as perplexity and sequence recovery rates.

#### A.7. Precision@K with regard to position and length

Figure 9 include ablation studies of SEIFER performance in term of precision according to relative positions and length of target sites in a protein.

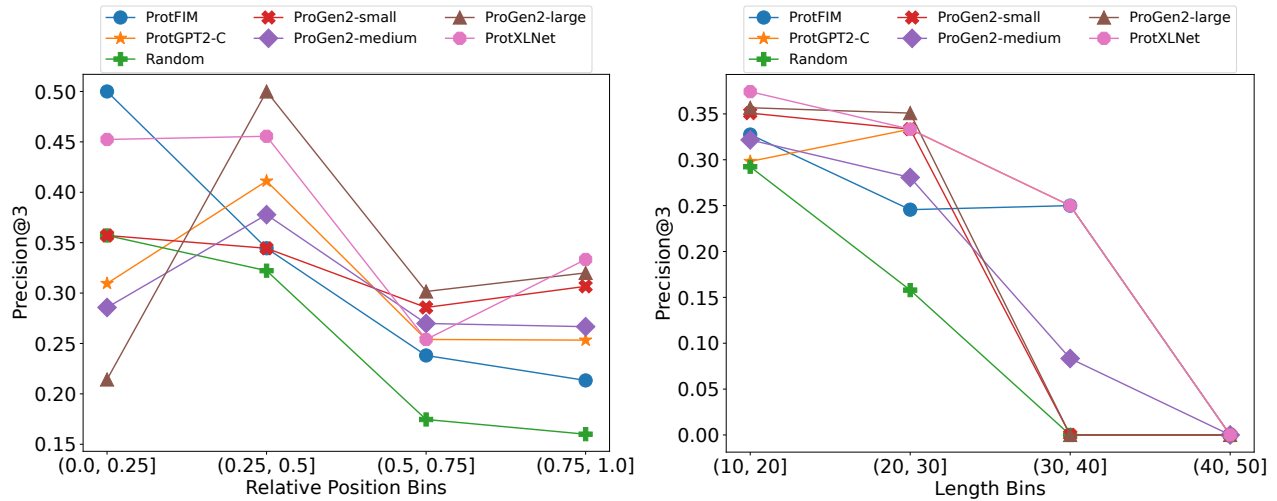


Figure 9. Performance changes in the metric of Precision@3 with regard to relative positions and length of middle sites.

#### A.8. FLIP

Table 5, 6, and 7 contain the zero-shot fitness prediction performances of various pLMs on three fitness landscapes.

Table 6. Zero-shot fitness prediction on adeno-associated virus GB1 landscape (Wu et al., 2016). All scores are Spearman correlation.

MODEL	#PARAMS	OBJECTIVE	1-VS-REST	2-VS-REST	3-VS-REST	LOW-VS-HIGH	AVG.
ESM-1B (MEAN)	750M	MLM	0.32	0.36	0.54	0.13	0.34
ESM-1V (MEAN)	750M	MLM	0.32	0.32	0.77	0.10	0.38
PROGEN2-SMALL	151M	CLM	-0.27	-0.30	-0.26	-0.03	-0.21
PROGEN2-MEDIUM	764M	CLM	-0.06	-0.16	-0.12	-0.10	-0.11
PROGEN2-LARGE	2.7B	CLM	0.19	0.28	0.44	0.06	0.24
PROTXLNET	409M	PLM	0.18	0.33	0.44	0.21	0.29
PROTGPT2-C	85M	CLM	0.02	0.05	0.44	0.20	0.18
PROTFIM	85M	FIM	0.01	0.18	0.63	0.18	0.25

Table 7. Zero-shot fitness prediction on the landscape from the Meltome Atlas (Jarzab et al., 2020). All scores are Spearman correlation.

MODEL	#PARAMS	OBJECTIVE	MIXED	HUMAN	HUMAN-CELL	AVG.
ESM-1B (MEAN)	750M	MLM	0.68	0.70	0.75	0.71
ESM-1V (MEAN)	750M	MLM	0.67	0.75	0.74	0.72
PROGEN2-SMALL	151M	CLM	0.46	0.63	0.59	0.56
PROGEN2-MEDIUM	764M	CLM	0.49	0.66	0.62	0.59
PROGEN2-LARGE	2.7B	CLM	0.67	0.70	0.66	0.68
PROTXLNET	409M	PLM	0.44	0.52	0.47	0.47
PROTGPT2-C	85M	CLM	0.49	0.55	0.54	0.53
PROTFIM	85M	FIM	0.51	0.66	0.63	0.60